ORIGINAL ARTICLE

AMERICAN JOURNAL OF
medical genetics PART A | **WILEY**

Pediatric pulmonary arterial hypertension due to a novel homozygous *GDF2* missense variant affecting BMP9 processing and activity

L. Chomette[1,2] 🔾 | E. Hupkens[3] | M. Romitti[2] 🔾 | L. Dewachter[3] 🔾 |
J. L. Vachiéry[1] 🔾 | S. Bailly[4] 🔾 | S. Costagliola[2] 🔾 | G. Smits[5] 🔾 | E. Tillet[4] 🔾 |
Antoine Bondue[1,2] 🔾

[1]Department of Cardiology, Hôpital Erasme, Hôpital Universitaire de Bruxelles, Université Libre de Bruxelles (ULB), Brussels, Belgium

[2]IRIBHM, Faculty of medicine, Université Libre de Bruxelles (ULB), Brussels, Belgium

[3]Laboratory of Physiology and Pharmacology (LAPP), Faculty of Medicine, Université Libre de Bruxelles (ULB), Brussels, Belgium

[4]Laboratory BioSanté, Université Grenoble Alpes, INSERM, CEA, Grenoble, France

[5]Department of Human Genetics, Hôpital Erasme, Hôpital Universitaire de Bruxelles, Université Libre de Bruxelles (ULB), Brussels, Belgium

Correspondence

Antoine Bondue, Department of Cardiology, Hôpital Erasme, Hôpital Universitaire de Bruxelles, Université Libre de Bruxelles, Brussels, Belgium.
Email: antoine.bondue@hubruxelles.be

Abstract

Pulmonary arterial hypertension (PAH) is a rare and severe disorder characterized by progressive pulmonary vasculopathy. *Growth differentiation factor* (*GDF*)2 encodes the pro-protein bone morphogenetic protein (BMP) 9, activated after cleavage by endoproteases into an active mature form. BMP9, together with BMP10, are high-affinity ligands of activin receptor-like kinase 1 (ALK1) and BMP receptor type II (BMPR2). *GDF2* mutations have been reported in idiopathic PAH with most patients being heterozygous carriers although rare homozygous cases have been described. The link between PAH occurrence and BMP9 or 10 expression level is still unclear. In this study, we describe a pediatric case of PAH also presenting with telangiectasias and epistaxis. The patient carries the novel homozygous *GDF2* c.946A > G mutation, replacing the first arginine of BMP9's cleavage site (R316) by a glycine. We show that this mutation leads to an absence of circulating mature BMP9 and mature BMP9-10 heterodimers in the patient's plasma although pro-BMP9 is still detected at a similar level as controls. In vitro functional studies further demonstrated that the mutation R316G hampers the correct processing of BMP9, leading to the secretion of inactive pro-BMP9. The heterozygous carriers of the variant were asymptomatic, similarly to previous reports, reinforcing the hypothesis of modifiers preventing/driving PAH development in heterozygous carriers.

KEYWORDS

BMP9, GDF2, hereditary hemorrhagic telangiectasia, pulmonary arterial hypertension

1 | INTRODUCTION

Pulmonary arterial hypertension (PAH) is a rare and severe disorder of the pulmonary vasculature, defined by an increased mean pulmonary artery pressure (mPAP) and pulmonary vascular resistance (PVR), in the absence of left heart pressure elevation (Humbert et al., 2022). A genetic

predisposition has been established in familial forms of PAH (Humbert et al., 2022). However, mutations can also be found in sporadic idiopathic PAH (IPAH) cases due to the reduced penetrance of the disease or de novo mutations (Morrell et al., 2019). Most PAH-associated genes are part of the transforming growth factor beta (TGF-β) signaling pathway, and *bone morphogenetic protein* (*BMP*) *receptor type II* (*BMPR2*) mutations are the most frequent (Morrell et al., 2019). Recently, mutations in *growth differentiation factor* (*GDF*) *2*, encoding BMP9, have also been associated

Tillet E. and Antoine Bondue contributed equally to this study.

with PAH. BMP9, together with BMP10, are high-affinity ligands of activin receptor-like kinase 1 (ALK1) encoded by *ACVRL1* (David et al., 2007). BMP9 is produced by hepatic stellate cells (Breitkopf-Heinlein et al., 2017; Tillet et al., 2018). It is synthesized as a homodimeric inactive precursor (pro-protein) and the mature form is produced after cleavage by pro-protein convertases at a consensus site comprising four basic amino acids [316]RRKR (Hosaka et al., 1991). Both unprocessed precursor (pro-BMP9) and mature BMP9 circulate in blood, but only mature BMP9 can activate ALK1, which subsequently forms a heterotetrameric complex with a type II receptor such as BMPR2 in endothelial cells (Desroches-Castan et al., 2022). Interestingly, BMP9 and BMP10 can be synthetized by hepatic stellate cells as BMP9-10 heterodimers (Tillet et al., 2018). In addition, it has been shown in mice that most of the circulating ALK1 activity can be attributed to BMP9-10 heterodimers since the loss of any of these two BMPs leads to a loss of ALK1-dependent activity in the plasma (Tillet et al., 2018). Numerous heterozygous *GDF2* mutations have been described in IPAH accounting for up to 1% of cases in European cohorts (Eyries et al., 2019; Gräf et al., 2018; Hodgson et al., 2020; Wang et al., 2019; Zhu et al., 2019), while only few carriers of homozygous *GDF2* mutations have been reported (Gallego et al., 2021; Hodgson et al., 2021; Liu et al., 2020; Upton et al., 2022; Wang et al., 2016). Interestingly, some are linked to PAH while others to hereditary hemorrhagic telangiectasia (HHT), and up to now, there have been no clues to better understand the factors regulating this distinction.

In this report, we identified a novel homozygous *GDF2* variant in a child diagnosed with PAH at 5 years of age in the context of recurrent respiratory infections. This variant affects the first arginine of BMP9's cleavage site (R316G). We demonstrate that this mutation hampers the correct maturation of BMP9 and leads to the loss of circulating mature BMP9 and BMP9-10 heterodimers, although pro-BMP9 is still secreted. This cleavage defect is also associated with an impairment of ALK1-dependent signaling.

2 | MATERIALS AND METHODS

2.1 | Editorial policies and ethical considerations

The Hospital-Faculty Ethics Committee of Academic Erasme Hospital (HUB, Brussels, Belgium) approved this study (P2018/611, A2020/250, A2021/081, A2021/162). Written informed consent was obtained from each participant and/or their legal representative, as appropriate, for all experiments involving human material. Written consent to publish anonymized clinical information was also obtained from the legal representatives of the patient.

2.2 | Genetic analysis

Genomic DNA was obtained from human peripheral whole blood according to usual laboratory procedures. Clinical exome sequencing of parent–child trio was performed (Novaseq6000, Illumina). BMP10 variants were excluded in the proband using Sanger sequencing. Multiplex

ligation-dependent probe amplification (MLPA) was performed for the genes *BMPR2*, *ENG* and *ACVRL1* using SALSA MLPA Probemix P093 HHT/HPAH (MRC-Holland BV, Amsterdam, NL), according to manufacturer's instructions. The MLPA products were analyzed using an 3130XL genetic analyzer (Applied Biosystems). Data analysis and interpretation were performed by the Coffalyser.Net software (MRC-Holland).

2.3 | Plasma sample collection

Blood samples were collected in EDTA pre-coated tubes, centrifuged, and plasma was stored at $-80°C$ until assayed.

2.4 | *ACVRL1* cloning

The entire coding sequence of *ACVRL1* was obtained using RNA from stem cell-derived endothelial cells (WA09, deposited at WiCell, https://www.wicell.org/) and cloned into a pcDNA3.1 vector. The entire *ACVRL1* sequence was verified by Sanger DNA sequencing.

2.5 | *GDF2*/BMP9 mutant generation

Human full length wild-type *GDF2* (encoding BMP9) and mutated *GDF2* carrying the [316]RQAA (R317Q, K318A, R319A) variant were cloned into a PCEP4 vector, as previously described (Tillet et al., 2018). Site-directed PCR-mutagenesis using PCEP4-*GDF2* as a template was performed using In-Fusion Cloning (Takara) to generate the following mutants: Q26X, R316G, R316S, and Y354RfsTer15. Q26X and Y354RfsTer15 are two previously reported homozygous *GDF2* mutants, while the R316S was described in a heterozygous carrier (Liu et al., 2020; G. Wang et al., 2016; Wang et al., 2019). All mutants were verified by Sanger DNA sequencing.

2.6 | Cell culture, transfection, and overexpression of mutants

HEK293T cells were transiently transfected using lipofectamine 2000 according to the manufacturer's instructions (ThermoFisher). Cells were grown for 24–48 h until confluency in Dulbecco's Modified Eagle Medium (DMEM) with 4.5 g/L glucose (Gibco) supplemented with 10% fetal bovine serum (FBS; Gibco) and penicillin/streptomycin (Gibco). Cells were then changed to serum-free medium and conditioned medium was collected after 24 h, filtered through a 0.2 μm filter, and stored at $-20°C$. Five independent batches were transfected and harvested for each BMP9 mutant.

2.7 | Enzyme-linked immunosorbent assay

ELISA detecting different BMP9 or BMP10 molecular forms were performed according to previously described protocols (Tillet

et al., 2018). The following antibody (Ab) couples were used, all purchased from R&D systems except when indicated.

(1) Capture anti-BMP9 Ab MAB3209/detection Ab BAF3209 for the measurement of mature/processed BMP9. (2) Capture anti-BMP9 prodomain Ab AF3879/detection Ab BAF3209 for the measurement of pro-BMP9 precursor. (3) Capture anti-BMP10 Ab (Duoset DY2926)/detection Ab BAF3956 for the measurement of pro-BMP10 precursor (4) capture home-made anti-BMP10 Ab clone 13C11/ detection Ab BAF3209 for the measurement of BMP9-10 heterodimers, as described in Tillet et al. (2018). Standard curves (0–1000 pg/mL) were obtained using recombinant BMP9 (Peprotech or R&D systems) or purified BMP9-10 (Tillet et al., 2018). Pro-BMP9 and pro-BMP10 ELISA levels are presented absorbance as no purified precursor forms are available for the standard curves. Five independent samples of conditioned media were diluted 1:100 to 1:1000 in phosphate buffered saline (PBS) containing 1% ultrapure BSA (Gibco) −0.1% Tween-20, and analyzed in duplicates. Plasma samples were diluted 1:2 in PBS-0.1% Tween 20%–0.5% triton-100, and analyzed in duplicates. ELISAs of plasma samples were repeated at least twice and values represent the mean of two independent experiments.

2.8 | Dual luciferase reporter gene assay

The reporter plasmid pGL3(BRE)$_2$-luc encoding firefly luciferase downstream of a BMP response element (BRE), part of the ID1 promoter, was kindly gifted by Martine Roussel and Peter ten Dijke (Addgene plasmid # 45126; http://n2t.net/addgene:45126; RRID:Addgene_45126) (Korchynskyi & ten Dijke, 2002). The Renilla luciferase plasmid pRL-SV40 was used as an internal control for transfection efficiency (Promega). NIH3T3 cells were transiently transfected using Lipofectamine 2000 (ThermoFisher), according to the manufacturer's instructions and based on a previously described protocol (David et al., 2007). Briefly, NIH3T3 cells were transfected with a mixture of 10 ng of pcDNA3-ALK1, 230 ng of pGL3(BRE)$_2$-luc and 20 ng of pRL-SV40-luc in Opti-MEM (Invitrogen) using lipofectamine 2000 (1 μL). After 4–6 h, cells were stimulated overnight with recombinant human BMP9 (Peprotech) or with diluted conditioned media (1:1000–1:20,000). Firefly and Renilla luciferase activities were measured sequentially with the Dual-Glo Luciferase reporter assay (Promega), on a luminometer (Centro LB 960, Berthold Technologies) with a 10-s integration time. Samples were tested in duplicates, in two independent experiments, for two different batches of conditioned media. Plasma samples' activity was recorded as previously described (Tillet et al., 2018). Briefly, firefly/renilla ratio obtained from non-stimulated wells were subtracted from the stimulated values of ALK1-transfected cells.

2.9 | Western blotting

Thirty microliters of conditioned media were separated on 10% SDS–PAGE under non-reducing or reducing conditions and blotted onto a

nitrocellulose membrane. Membranes were blocked in 5% non-fat milk in Tris-buffered saline (TBS) for 1 h at RT and probed overnight at 4°C with an anti-BMP9 prodomain antibody (AF3879, R&D systems, 1:1000) followed by a secondary rabbit anti-goat IgG antibody (Promega). Membranes were revealed with LumiGLO reagent substrate (Cell Signaling) and captured with an Azure 500 system (Azure Biosystems).

2.10 | Statistical analysis

Data are expressed as mean or median according to the distribution. Statistical analysis was performed using GraphPad Prism 8.0.2. Statistical significance was assessed using a two-tailed unpaired Mann–Whitney test and data are presented as median ± interquartile range (IQR). Significance levels were assessed between wild-type BMP9 and each BMP9 mutant. p-Values <0.05 were considered statistically significant.

3 | RESULTS

3.1 | Clinical description

We report the case of a 9-year-old female diagnosed with PAH. She was born at 37 weeks of gestation after an uneventful pregnancy. The pedigree of the family is presented in Figure 1. Her parents are first-degree cousins of Turkish origin (III-1 and III-2), and both are healthy. They lost a first child, a boy born at 35 weeks of gestation, who died at 3.5 years old (IV-1) from a cardiac arrest of unknown etiology. Also, a female fetus died in utero at 7–8 months (IV-2). Hydrops fetalis was observed and a cardiomyopathy of unknown etiology was suspected according to old reports, but no further details were available. No DNA was available for both cases. In addition, the mother had multiple miscarriages. Finally, the patient has a 15-year-old sister in good health (IV-3).

The patient (IV-4) had two episodes of bronchopneumonia during her fourth year and was hospitalized for the second episode. Asthenia and dyspnea on exertion were also noticed at that time. A chest CT was performed showing large pulmonary arteries without other anomalies. Transthoracic echocardiography revealed a normal anatomy except for a patent *foramen ovale*. Right heart catheterization was performed highlighting a mPAP of 48 mmHg, a right atrial pressure of 12 mmHg and a pulmonary artery wedge pressure of 9 mmHg. At ambient air, her arterial oxygen saturation was measured at 95% and her venous saturation at 69%. Arteriography showed a normal arborization of pulmonary arteries and no venous anomaly. Chest CT angiography excluded pulmonary embolism and abnormal venous return. An abdominal ultrasound did not reveal vascular abnormalities. Based on this, the patient was diagnosed with group 1 PAH. She was first treated with sildenafil, followed by dual oral therapy with the addition of bosentan. The patient has been stable on this treatment regimen for the past 5 years, and is
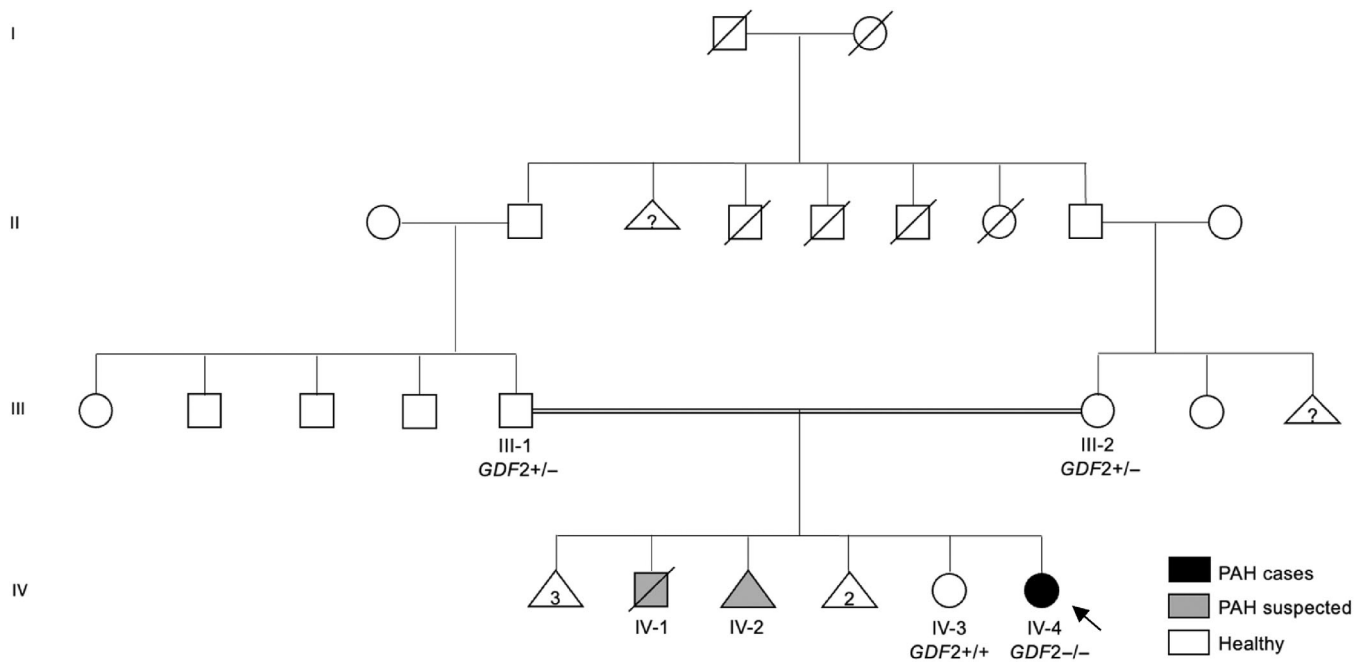
FIGURE 1 Multigenerational family pedigree. Family member IV-4 is the only documented case of PAH. Two members died at very young ages (3.5 years old and in utero) due to unclear etiologies (IV-1 and IV-2, respectively), for whom PAH and/or a cardiomyopathy was subsequently suspected. Both parents are asymptomatic heterozygous carriers (III-1 and III-2). The older sister is not a carrier (IV-3). There were many miscarriages in each generation (triangles). The double line represents consanguinity. $+/+$ represents wild-type *GDF2*, $+/-$ represents heterozygous carriers of the R316G *GDF2* variant and $-/-$ represents homozygous carriers of the variant. $\square$ = male, $\bigcirc$ = female.

currently in the low risk category according to ESC guidelines (Humbert et al., 2022).

In addition to PAH, rare thin horizontal telangiectasias were observed on the patient's cheeks and few pin-points telangiectasias were observed on her forearms after careful skin examination at 9 years old. No telangiectasia was observed on the lips or oral cavity. The patient also had a history of recurrent epistaxis.

In this context of childhood-onset PAH in a consanguineous family, clinical exome sequencing of parent–child trio was performed. This analysis revealed the presence of the *GDF2* c.946A > G (p.Arg316Gly) variant in the homozygous state in the patient (Figure S1). Both parents were heterozygous carriers (Figure S1) while the unaffected sister (IV-3) was not a carrier (Figure 1). There was no familial history suggestive of PAH or HHT (Figure 1). All family members underwent brain magnetic resonance imaging and no cerebral vascular anomalies were detected.

The *GDF2* c.946A > G (p.Arg316Gly) variant was not reported in gnomAD (https://gnomad.broadinstitute.org) and occurs at a position that is conserved across species (https://genome.ucsc.edu/).(Karczewski et al., 2020; Kent et al., 2002) It has not been previously reported in the literature or ClinVar (https://www.ncbi.nlm.nih.gov/clinvar/). The variant induces a change of amino acid from an Arginine, a positively charged amino acid, to a Glycine, one of the three special amino acids. The SIFT score predicts a damaging effect while the Combined Annotation Dependent Depletion (CADD) score is of 23.9 (Table S1) (Ng & Henikoff, 2001; Rentzsch et al., 2019).

3.2 | BMP9 and BMP10 circulating forms in plasma

Because the BMP9 R316G variant induces a change of the first amino acid of the furin cleavage site (^{316}RRKR) of pro-BMP9, we assessed the circulating levels of both BMP9's processed mature and precursor forms using specific ELISAs, as previously described (Tillet et al., 2018). Plasma samples from the index case, from first-degree relatives (parents and sister), and from age-matched controls (age 7–54 years old) were collected.

Mature BMP9 ELISA detects the mature growth factor domain, whether it remains associated to the prodomain (pro-complex BMP9) or not (Figure S2). Conversely, ELISA for pro-BMP9 only measures the precursor form and does not detect pro-complex BMP9 (Figure S2) (Hodgson et al., 2020; Kienast et al., 2016). As shown in Figure 2a, mature BMP9 was not detectable in the plasma of the patient carrying the homozygous mutation R316G, while the heterozygous parents both had a detectable level, although lower than the healthy control group. In contrast, the level of the sister, who did not carry any mutation, was quite high, even higher than all controls. Regarding the precursor form, pro-BMP9 was detected in the homozygous patient's plasma at a similar level than controls, indicating that BMP9 was normally expressed but unprocessed (Figure 2b). Again, the unaffected sister had a higher level of pro-BMP9. BMP9 and BMP10 can form a heterodimer, detected by a specific ELISA using an anti-BMP10 as a capture antibody and an anti-BMP9 antibody for detection (Tillet et al., 2018). As expected, there was no detectable
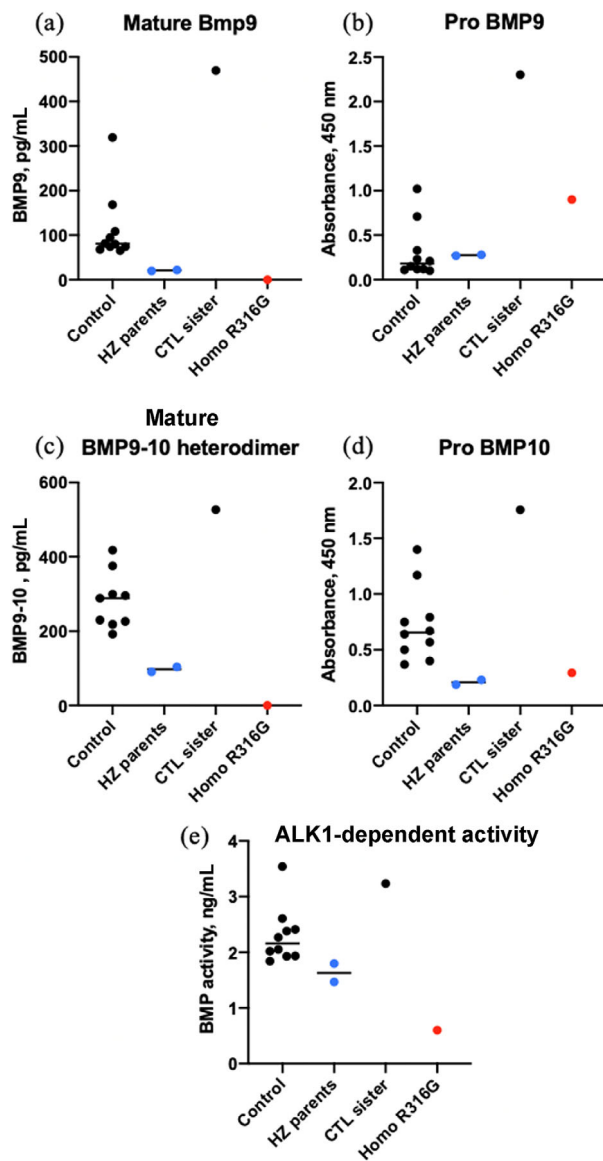
FIGURE 2 Homozygous *GDF2* R316G variant leads to a loss of circulating processed BMP9. Levels of (a) mature BMP9, (b) precursor pro-BMP9, (c) mature BMP9-10 heterodimer, and (d) precursor pro-BMP10 were measured with specific ELISAs in the plasma of 10 control donors, in the R316G heterozygous (HZ) parents, the wild-type sister (CTL-sister), and the R316G homozygous index case (Homo R316G). (e) ALK1-dependent BRE activity in ALK1-transfected NIH3T3 cells. Cells were stimulated overnight with 1% plasma and the relative luciferase activity was quantified using recombinant BMP9 as the standard. Firefly luciferase activity was normalized to Renilla luciferase activity. Samples were tested in duplicates. All data are expressed as the mean value of two independent experiments. The bar represents the mean value of all controls or of both parents.

circulating mature BMP9-10 heterodimers in the patient's plasma, while the heterozygous parents had lower circulating levels than healthy controls, suggesting haploinsufficiency (Figure 2c). Because it was reported that BMP10 circulating levels can also be altered by the presence of *GDF2* mutations (Hodgson et al., 2020), we aimed to

determine circulating mature BMP10 levels. As circulating mature BMP10 levels were below the ELISA detection limit, we could only measure pro-BMP10 circulating levels. As for BMP9, this ELISA recognizes the precursor unprocessed BMP10 and not pro-complex BMP10 (Figure S3). We found that pro-BMP10 was detectable in the plasma of the homozygous patient, although at a lower level than in controls (Figure 2d). The heterozygous parents also had lower levels of circulating pro-BMP10 than healthy controls, and again, the unaffected sister had a higher circulating level (Figure 2d).

Circulating forms of BMP9 and BMP10 are mostly biologically active as a BMP9-10 heterodimeric form (Tillet et al., 2018). We therefore tested the capacity of the patient's plasma to activate ALK1-mediated Smad signaling through a BMP-responsive element (BRE) luciferase assay in NIH3T3 cells. In accordance with the ELISA data, we found that the plasma sample of the homozygous patient had a very low biological activity compared to healthy controls or to the heterozygous parents (Figure 2e). We assumed that the measured activity was only the product of ALK1 stimulation since cells that are not transfected with ALK1 do not display any measurable activity (Figure S4).

3.3 | *GDF2* R316G mutation impairs BMP9 processing and activation

To characterize the impact of the R316G variant on BMP9 processing and activation *in vitro*, we generated a vector expressing the mutant form of BMP9 (R136G), as well as vectors containing previously described mutations associated with either PAH or HHT for comparison (Figure 3a). The Q26X homozygous nonsense mutation was reported in a 5-year-old patient with IPAH and was shown to result in a BMP9 secretion defect (Hodgson et al., 2021; Wang et al., 2016). The Y354RfsTer15 homozygous variant was described in a pediatric HHT case but no functional studies were performed (Liu et al., 2020). In addition, we chose to analyze the R316S mutation described as a heterozygous variant in an IPAH case (Wang et al., 2019). All variants were generated by site directed mutagenesis (Table S2) using PCEP4 encoding human BMP9 as a template (Tillet et al., 2018). They were all independently transfected in HEK293T cells and each serum-free conditioned media were assessed for BMP9 production, maturation and activity. As a control, we used the previously described BMP9 [316]RQAA mutant which abolishes the processing of pro-BMP9 (Tillet et al., 2018).

ELISA directed against mature BMP9 demonstrated that the R316G mutation resulted in an almost complete absence of processed mature BMP9, similarly to the BMP9 [316]RQAA mutant (Figure 3b). Identical results were obtained with the R316S mutant, highlighting the importance of the first arginine of the cleavage site for BMP9 processing. The nonsense mutations Q26X and Y354RfsTer15 could not be detected, in accordance with the total absence of secretion of these mutants.

Interestingly, pro-BMP9 could be detected in R316G conditioned media at a similar level as the BMP9 [316]RQAA unprocessed control, while, as expected, none was detected for WT BMP9 which was
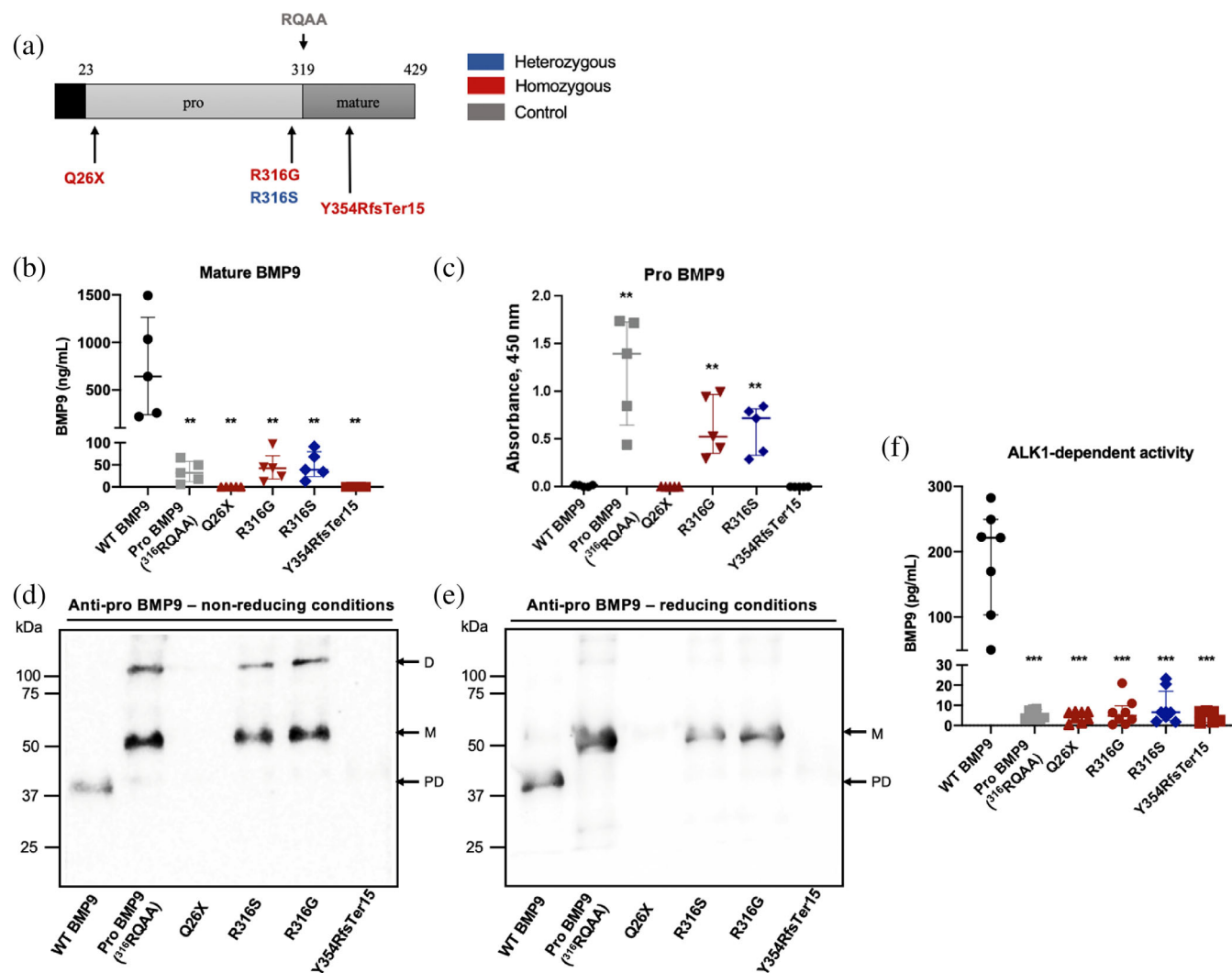
FIGURE 3 The *GDF2* R316G mutation leads to the production of unprocessed nonfunctional BMP9. (a) Schematic representation of BMP9 domains and location of the studied mutations: Q26X, R316G, R316S, and Y354RfsTer15. The previously described BMP9 [316]RQAA mutant (Pro BMP9) was used as a control for pro-protein cleavage deficiency (Tillet et al., 2018). (b, c) ELISA quantification of (b) mature BMP9 and (c) pro-BMP9. Conditioned media from 5 independent experiments were used and each sample was analyzed in duplicates. (d, e) Western blot analysis of conditioned media from HEK293T cells overexpressing wild-type or mutant BMP9 using an antibody targeting human BMP9 propeptide (AF3879, R&D systems) in (d) non-reducing and (e) reducing conditions. D: dimer (110 kDa), M: monomer (55 kDa), and PD: prodomain (40 kDa). (f) ALK1-dependent BRE activity in ALK1-transfected NIH3T3 cells. Cells were stimulated overnight with conditioned media (diluted 1:5000) and the relative luciferase activity was quantified using recombinant BMP9 as the standard. Firefly luciferase activity was normalized to Renilla luciferase activity. Samples were tested in duplicates, in two independent experiments, for two different batches of conditioned media. (b, c, f) Data are presented as median ± interquartile range (IQR). *p*-Values were calculated using Mann–Whitney test by comparing wild-type to mutants. *$p < 0.05$, **$p < 0.01$, ***$p < 0.001$.

entirely cleaved (Figure 3c). Again, identical results were obtained with the R316S mutant. This confirms that the R316G and R316S mutants are secreted and unprocessed. In contrast, a secretion defect of Q26X and Y354RfsTer15 was further confirmed since the precursor form was totally absent from the conditioned media of those mutants (Figure 3c).

Western blot analysis using an antibody against BMP9 prodomain confirmed that R316 is necessary for BMP9 processing (Figure 3d, e). BMP9's cleaved prodomain (40 kDa) could only be detected in conditioned media from WT BMP9. R316G and R316S showed a similar electrophoretic profile as the BMP9 [316]RQAA unprocessed mutant (pro-BMP9), with a mixture of dimeric and monomeric unprocessed BMP9 (110 and 55 kDa, respectively) under non-reducing conditions (Figure 3d), that are, as expected, converted to a 55 kDa band after reduction (Figure 3e).

Finally, we assessed the mutants' ability to activate the ALK1 pathway in a BRE luciferase assay using conditioned media (Figure 3f). As expected, similarly to the other mutants, R316G had an extremely low activity compared to WT BMP9, demonstrating that this mutation leads to the production of an inactive BMP9 ligand.

TABLE 1 Summary of reported homozygous or compound heterozygous *GDF2* mutations identified in pediatric cases.

DNA mutation	Protein substitution	Age at diagnosis	Sex and ethnicity	Family history	Clinical description	Suggested mechanism	Circulating BMP9 or10	References
c.76C > T	p.Q26X	5 years	Mexican male	None	IPAH and telangiectasias	No secretion	No BMP9/ no BMP10	Wang et al., 2016; Hodgson et al., 2021; this study
c.328C > T	p.R110W	5 years	Spanish male	None	IPAH-epistaxis and telangiectasias	Reduced stability	nd	Gallego et al., 2021; Hodgson et al., 2020
c.445G > A + del q11.22–q11.23[a]	p.E149K	4 years	Spanish female	None	IPAH	nd	nd	Gallego et al., 2021
c.1060_1062delinsAG	p.Y354RfsTer15	5 years	Chinese male	Epistaxis	HHT-like: PAVM, epistaxis and telangiectasias	No secretion	nd	Liu et al., 2020; this study
c.958A > T[b]	p.S320C	3 months	Male	None	IPAH	Processing defect	No BMP9/ low BMP10	Upton et al., 2022; Hodgson et al., 2020
c.958A > T[b]	p.S320C	4 years	Female	None	IPAH	Processing defect	No BMP9/ low BMP10	Upton et al., 2022; Hodgson et al., 2020
c.835G > T	p.E279X	9 years	Female	None	HHT-like: PAVM-epistaxis and telangiectases	nd	No BMP9/ no BMP10	Hodgson et al., 2021
c.451C > T	p.R151X	Birth	Female	Hydrops-miscarriages	Lymphatic dysplasia-hydrops fetalis	nd	nd	Aukema et al., 2020
c.946A > G	p.R316G	5 years	Turkish female	None	IPAH-epistaxis and telangiectases	Processing defect	No BMP9/ low BMP10	This study

Note: Suggested mechanisms are derived from *in vitro* data. Circulating BMP9 or 10 plasma levels identified by ELISA.

Abbreviations: HHT, hereditary hemorrhagic telangiectasia; IPAH, idiopathic pulmonary arterial hypertension; Nd, not determined; PAVM, pulmonary arterio-venous malformation.

[a]Compound heterozygous mutations.

[b]Both cases are siblings.

4 | DISCUSSION

Using clinical exome sequencing in trio (index case and parents), we identified the novel missense variant c.946A > G (p.Arg316Gly) of the *GDF2* gene, located at the cleavage site of its encoded pro-protein BMP9. BMP9 is the ligand of the ALK1/BMPR2 signaling pathway, the main pathway implicated in PAH (Morrell et al., 2019). Heterozygous *GDF2* mutations were found in up to about 6% of cases in a Chinese cohort of IPAH patients, where *GDF2* ranked as the second most mutated gene after *BMPR2* (Wang et al., 2019). *GDF2* mutations were also reported in a French cohort at a frequency of 1.2% in PAH cases (two sporadic cases) and in a European cohort at a lower frequency of 0.8% (Eyries et al., 2019; Gräf et al., 2018). The case we report here is a homozygous carrier of the R316G variant located within the

cleavage site of the BMP9 precursor. The patient was diagnosed with PAH at 5 years old, with recurrent epistaxis and few thin telangiectasias on her cheeks on careful physical examination at the age of 9 years old, after variant identification. Epistaxis and telangiectasia are reminiscent of another disease linked to the BMP9 signaling axis: HHT. In HHT, it is most often the BMP9 receptor (ALK1) or the co-receptor (ENG) that are mutated, although rare *GDF2* mutations were first associated with a syndrome resembling HHT with vascular abnormalities (Wooderchak-Donahue et al., 2013). Beside our case, there are rare reports of homozygous or compound heterozygous *GDF2*-mutation carriers presenting with either a HHT-like syndrome or PAH, with or without telangiectasias (summarized in Table 1) (Gallego et al., 2021; Hodgson et al., 2021; Liu et al., 2020; Upton et al., 2022; Wang et al., 2016). However, the underlying mechanisms leading to

one disease instead of the other are still unknown (Ormiston et al., 2019).

One way to better characterize the pathogenicity of the R316G variant is to assess BMP9 circulating level. In this report, we show that the level of circulating mature BMP9 in the index case is not detectable while the level of precursor BMP9 was comparable to healthy controls. In addition, through thorough *in vitro* testing, we demonstrated that the mutation hampers BMP9 processing but not the biosynthesis and secretion of the protein. The lack of BMP9 processing is correlated to a highly reduced plasma-derived BMP activity in the index case. Since the variant R316G affects the first amino acid of BMP9's cleavage site, impaired processing was expected. However, Balanchandar et al. demonstrated that other variants, located away from the cleavage site, could also lead to a processing deficiency, such as the p.Cys428Arg variant (Balachandar et al., 2022).

Both heterozygous parents are asymptomatic although they present with a low mature BMP9 plasmatic level, but this could be explained by a preserved BMP-signaling activity. In this regard, Hodgson et al. showed that plasma samples of heterozygous asymptomatic carriers of the E279X mutation had a preserved serum activity despite reduced mature BMP9 levels, while the homozygous carrier had a drastically reduced activity (Hodgson et al., 2021). On the other hand, it has been shown that the R110W *GDF2* mutation can cause the development of PAH in heterozygous carriers (Hodgson et al., 2020), whereas the same mutation is asymptomatic in the heterozygous parents of a pediatric PAH patient carrying the mutation in the homozygous state (Gallego et al., 2021). Interestingly, heterozygous patients developing PAH had a reduced BMP9 level and activity, indicating that the BMP9 level could be an important driver for the development of PAH (Hodgson et al., 2020). These results point toward an incomplete penetrance of BMP9 variants, including the one described in this report, and the need for a second hit, genetic or environmental, to develop the disorder (Gallego et al., 2021; Upton et al., 2022). Furthermore, Hodgson et al. demonstrated that heterozygous *GDF2* mutation carriers were older and presented with less severe hemodynamics than *BMPR2* mutation carriers, which is in line with the need for a second hit in heterozygous cases (Hodgson et al., 2020). Of note, the wild-type sibling in this report had one of the highest BMP activity compared to controls. This could potentially be age and/or gender dependent. We could also hypothesize that protective modifiers implicated in ALK1-dependent signaling run in the family to prevent disease expression in the heterozygous carriers, explaining such a high level of mature BMP9 and ALK-1-dependent signaling in the wild-type sister, although this can only be a speculation at this time.

In addition to BMP9 level, plasmatic BMP10 level is an important factor to determine, since it has been shown that both BMP levels are highly correlated (Hodgson et al., 2020). This is likely due to the fact that the BMP9-BMP10 heterodimeric form is the main active form in plasma (Tillet et al., 2018). Consistently with the loss of mature BMP9, we show that BMP9-10 heterodimers are no longer detected in the plasma of the R316G homozygous patient, which also explains the loss of plasma ALK1-dependent activity in this patient. It can be

assumed that mutated pro-BMP9 can heterodimerize with BMP10 but whether this heterodimerization would affect BMP10 processing, or whether a hybrid pro-BMP9-BMP10 heterodimer could be responsible for the remaining activity observed in the patient's plasma, needs to be determined.

To assess BMP10 level, we used an ELISA detecting pro-BMP10 since ELISA for mature BMP10 was not sensitive enough, even for control samples, as already described (Hodgson et al., 2020). We show a rather low but detectable pro-BMP10 level, both in the index case and heterozygous parents, in contrast to what was shown in two previously described homozygous patients (Q26X and E279X carriers— Table 1) (Hodgson et al., 2021). Two other cases of pediatric PAH have recently been described in which a low level of BMP10 was measured, similarly to the patient in our study (Table 1- Upton et al., 2022). Of note, both variants for which BMP10 levels were undetectable were nonsense variants, while other cases (including this report) with low BMP10 levels carried missense variants (Table 1). We cannot exclude an effect of the type of substitution on remaining BMP10 levels in this context. Upton et al. proposed that the presence of circulating BMP10 in some PAH patients may protect against the occurrence of telangiectasias in addition to PAH (Upton et al., 2022). However, our results contradict this hypothesis since the patient in our study also presented with telangiectasias.

Additionally, an association between *hydrops fetalis* and the homozygous *GDF2* variant R151X has been reported (Aukema et al., 2020). Interestingly, in the present case, there was a history of intrauterine fetal demise in the late stages of pregnancy in the context of hydrops with a suspected cardiomyopathy. However, no detailed reports nor DNA samples were available for this fetus. The family described in this report also had a strong history of miscarriages. Additional genetic studies are being performed to exclude other etiologies due to consanguinity but we cannot exclude that the *GDF2* mutation could lead to a vasculopathy of the placenta, as ALK-1 has been implicated in placental vasculature development (Hong et al., 2007).

Overall, we identified a novel homozygous *GDF2* variant, R316G, affecting BMP9's cleavage domain and leading to childhood-onset PAH with epistaxis and rare telangiectasias of the cheeks. We demonstrated that R316G hampers the correct processing of BMP9, leading to the loss of mature BMP9 and BMP9-BMP10 heterodimers, and to an impairment of ALK1-dependent signaling. Furthermore, the heterozygous carriers of the variant in this family were asymptomatic, similarly to previous reports, reinforcing the hypothesis of modifiers preventing/driving PAH development in heterozygous carriers.

AUTHOR CONTRIBUTIONS

CONFLICT OF INTEREST STATEMENT

The authors declare no conflict of interest.

DATA AVAILABILITY STATEMENT

The data that support the findings of this study are available from the corresponding author upon reasonable request.

ORCID

L. Chomette https://orcid.org/0000-0002-8227-9281

M. Romitti https://orcid.org/0000-0003-1402-7266

L. Dewachter https://orcid.org/0000-0002-0452-1861

J. L. Vachiéry https://orcid.org/0000-0002-6358-7852

S. Bailly https://orcid.org/0000-0003-1043-7030

S. Costagliola https://orcid.org/0000-0002-6869-9941

G. Smits https://orcid.org/0000-0003-2845-6758

E. Tillet https://orcid.org/0000-0002-0076-8007

Antoine Bondue https://orcid.org/0000-0002-4103-515X

REFERENCES

Aukema, S. M., ten Brinke, G. A., Timens, W., Vos, Y. J., Accord, R. E., Kraft, K. E., Santing, M. J., Morssink, L. P., Streefland, E., Diemen, C. C., Vrijlandt, E. J., Hulzebos, C. V., & Kerstjens-Frederikse, W. S. (2020). A homozygous variant in growth and differentiation factor 2 (*GDF2*) may cause lymphatic dysplasia with hydrothorax and nonimmune hydrops fetalis. *American Journal of Medical Genetics Part A*, *182*(9), 2152–2160. https://doi.org/10.1002/ajmg.a.61743

Balachandar, S., Graves, T. J., Shimonty, A., Kerr, K., Kilner, J., Xiao, S., Slade, R., Sroya, M., Alikian, M., Curetean, E., Thomas, E., McConnell, V. P. M., McKee, S., Boardman-Pretty, F., Devereau, A., Fowler, T. A., Caulfield, M. J., Alton, E. W., Ferguson, T., … Shovlin, C. L. (2022). Identification and validation of a novel pathogenic variant in GDF2 (BMP9) responsible for hereditary hemorrhagic telangiectasia and pulmonary arteriovenous malformations. *American Journal of Medical Genetics. Part A*, *188*(3), 959–964. https://doi.org/10.1002/ajmg.a.62584

Breitkopf-Heinlein, K., Meyer, C., König, C., Gaitantzi, H., Addante, A., Thomas, M., Wiercinska, E., Cai, C., Li, Q., Wan, F., Hellerbrand, C., Valous, N. A., Hahnel, M., Ehlting, C., Bode, J. G., Müller-Bohl, S., Klingmüller, U., Altenöder, J., Ilkavets, I., … ten Dijke, P. (2017). BMP-9 interferes with liver regeneration and promotes liver fibrosis. *Gut*, *66*(5), 939–954. https://doi.org/10.1136/gutjnl-2016-313314

David, L., Mallet, C., Mazerbourg, S., Feige, J.-J., & Bailly, S. (2007). Identification of BMP9 and BMP10 as functional activators of the orphan activin receptor-like kinase 1 (ALK1) in endothelial cells. *Blood*, *109*(5), 1953–1961. https://doi.org/10.1182/blood-2006-07-034124

Desroches-Castan, A., Tillet, E., Bouvard, C., & Bailly, S. (2022). BMP9 and BMP10: Two close vascular quiescence partners that stand out. *Developmental Dynamics*, *251*(1), 158–177. https://doi.org/10.1002/dvdy.395

Eyries, M., Montani, D., Nadaud, S., Girerd, B., Levy, M., Bourdin, A., Trésorier, R., Chaouat, A., Cottin, V., Sanfiorenzo, C., Prevot, G., Reynaud-Gaubert, M., Dromer, C., Houeijeh, A., Nguyen, K., Coulet, F., Bonnet, D., Humbert, M., & Soubrier, F. (2019). Widening the landscape of heritable pulmonary hypertension mutations in paediatric and adult cases. *European Respiratory Journal*, *53*(3), 1801371. https://doi.org/10.1183/13993003.01371-2018

Gallego, N., Cruz-Utrilla, A., Guillén, I., Bonora, A. M., Ochoa, N., Arias, P., Lapunzina, P., Escribano-Subias, P., Nevado, J., & Tenorio-Castaño, J. (2021). Expanding the evidence of a semi-dominant inheritance in GDF2 associated with pulmonary arterial hypertension. *Cell*, *10*(11), 3178. https://doi.org/10.3390/cells10113178

Gräf, S., Haimel, M., Bleda, M., Hadinnapola, C., Southgate, L., Li, W., Hodgson, J., Liu, B., Salmon, R. M., Southwood, M., Machado, R. D., Martin, J. M., Treacy, C. M., Yates, K., Daugherty, L. C., Shamardina, O., Whitehorn, D., Holden, S., Aldred, M., … Morrell, N. W. (2018). Identification of rare sequence variation underlying heritable pulmonary arterial hypertension. *Nature Communications*, *9*(1), 1416. https://doi.org/10.1038/s41467-018-03672-4

Hodgson, J., Ruiz-Llorente, L., McDonald, J., Quarrell, O., Ugonna, K., Bentham, J., Mason, R., Martin, J., Moore, D., Bergstrom, K., Bayrak-Toydemir, P., Wooderchak-Donahue, W., Morrell, N. W., Condliffe, R., Bernabeu, C., & Upton, P. D. (2021). Homozygous *GDF2* nonsense mutations result in a loss of circulating BMP9 and BMP10 and are associated with either PAH or an "HHT-like" syndrome in children. *Molecular Genetics & Genomic Medicine*, *9*(12), e1685. https://doi.org/10.1002/mgg3.1685

Hodgson, J., Swietlik, E. M., Salmon, R. M., Hadinnapola, C., Nikolic, I., Wharton, J., Guo, J., Liley, J., Haimel, M., Bleda, M., Southgate, L., Machado, R. D., Martin, J. M., Treacy, C. M., Yates, K., Daugherty, L. C., Shamardina, O., Whitehorn, D., Holden, S., … Morrell, N. W. (2020). Characterization of *GDF2* mutations and levels of BMP9 and BMP10 in pulmonary arterial hypertension. *American Journal of Respiratory and Critical Care Medicine*, *201*(5), 575–585. https://doi.org/10.1164/rccm.201906-1141OC

Hong, K.-H., Seki, T., & Oh, S. P. (2007). Activin receptor-like kinase 1 is essential for placental vascular development in mice. *Laboratory Investigation*, *87*(7), 670–679. https://doi.org/10.1038/labinvest.3700560

Hosaka, M., Nagahama, M., Kim, W. S., Watanabe, T., Hatsuzawa, K., Ikemizu, J., Murakami, K., & Nakayama, K. (1991). Arg-X-Lys/Arg-Arg motif as a signal for precursor cleavage catalyzed by furin within the constitutive secretory pathway. *The Journal of Biological Chemistry*, *266*(19), 12127–12130.

Humbert, M., Kovacs, G., Hoeper, M. M., Badagliacca, R., Berger, R. M. F., Brida, M., Carlsen, J., Coats, A. J. S., Escribano-Subias, P., Ferrari, P., Ferreira, D. S., Ghofrani, H. A., Giannakoulas, G., Kiely, D. G., Mayer, E., Meszaros, G., Nagavci, B., Olsson, K. M., Pepke-Zaba, J., … Wort, S. J. (2022). ESC/ERS guidelines for the diagnosis and treatment of pulmonary hypertension. *European Heart Journal*, *43*(38), 3618–3731. https://doi.org/10.1093/eurheartj/ehac237

Karczewski, K. J., Francioli, L. C., Tiao, G., Cummings, B. B., Alföldi, J., Wang, Q., Collins, R. L., Laricchia, K. M., Ganna, A., Birnbaum, D. P., Gauthier, L. D., Brand, H., Solomonson, M., Watts, N. A., Rhodes, D., Singer-Berk, M., England, E. M., Seaby, E. G., Kosmicki, J. A., … MacArthur, D. G. (2020). The mutational constraint spectrum quantified from variation in 141,456 humans. *Nature*, *581*(7809), 434–443. https://doi.org/10.1038/s41586-020-2308-7

Kent, W. J., Sugnet, C. W., Furey, T. S., Roskin, K. M., Pringle, T. H., Zahler, A. M., & Haussler, D. (2002). The human genome browser at UCSC. *Genome Research*, *12*(6), 996–1006. https://doi.org/10.1101/gr.229102

Kienast, Y., Jucknischke, U., Scheiblich, S., Thier, M., de Wouters, M., Haas, A., Lehmann, C., Brand, V., Bernicke, D., Honold, K., & Lorenz, S. (2016). Rapid activation of bone Morphogenic protein 9 by receptor-mediated displacement of pro-domains. *Journal of Biological Chemistry*, *291*(7), 3395–3410. https://doi.org/10.1074/jbc.M115.680009

Korchynskyi, O., & ten Dijke, P. (2002). Identification and functional characterization of distinct critically important bone morphogenetic protein-specific response elements in the Id1 promoter. *Journal of Biological Chemistry*, *277*(7), 4883–4891. https://doi.org/10.1074/jbc.M111023200

Liu, J., Yang, J., Tang, X., Li, H., Shen, Y., Gu, W., & Zhao, S. (2020). Homozygous *GDF2* -related hereditary hemorrhagic telangiectasia in a Chinese family. *Pediatrics*, *146*(2), e20191970. https://doi.org/10.1542/peds.2019-1970

Morrell, N. W., Aldred, M. A., Chung, W. K., Elliott, C. G., Nichols, W. C., Soubrier, F., Trembath, R. C., & Loyd, J. E. (2019). Genetics and genomics of pulmonary arterial hypertension. *European Respiratory Journal*, *53*(1), 1801899. https://doi.org/10.1183/13993003.01899-2018

Ng, P. C., & Henikoff, S. (2001). Predicting deleterious amino acid substitutions. *Genome Research*, *11*(5), 863–874. https://doi.org/10.1101/gr.176601

Ormiston, M. L., Godoy, R. S., Chaudhary, K. R., & Stewart, D. J. (2019). The Janus faces of bone morphogenetic protein 9 in pulmonary arterial hypertension: Friend and foe? *Circulation Research*, *124*(6), 822–824. https://doi.org/10.1161/CIRCRESAHA.119.314753

Rentzsch, P., Witten, D., Cooper, G. M., Shendure, J., & Kircher, M. (2019). CADD: Predicting the deleteriousness of variants throughout the human genome. *Nucleic Acids Research*, *47*(D1), D886–D894. https://doi.org/10.1093/nar/gky1016

Tillet, E., Ouarné, M., Desroches-Castan, A., Mallet, C., Subileau, M., Didier, R., Lioutsko, A., Belthier, G., Feige, J.-J., & Bailly, S. (2018). A heterodimer formed by bone morphogenetic protein 9 (BMP9) and BMP10 provides most BMP biological activity in plasma. *Journal of Biological Chemistry*, *293*(28), 10963–10974. https://doi.org/10.1074/jbc.RA118.002968

Upton, P., Richards, S., Bates, A., Niederhoffer, K. Y., Morrell, N. W., & Christian, S. (2022). A rare homozygous missense GDF2 (BMP9) mutation causing PAH in siblings: Does BMP10 status contribute? *American Journal of Medical Genetics. Part A*, *191*, 228–233. https://doi.org/10.1002/ajmg.a.62996

Wang, G., Fan, R., Ji, R., Zou, W., Penny, D. J., Varghese, N. P., & Fan, Y. (2016). Novel homozygous BMP9 nonsense mutation causes pulmonary arterial hypertension: A case report. *BMC Pulmonary Medicine*, *16*(1), 17. https://doi.org/10.1186/s12890-016-0183-7

Wang, X.-J., Lian, T.-Y., Jiang, X., Liu, S.-F., Li, S.-Q., Jiang, R., Wu, W.-H., Ye, J., Cheng, C.-Y., Du, Y., Xu, X.-Q., Wu, Y., Peng, F.-H., Sun, K., Mao, Y.-M., Yu, H., Liang, C., Shyy, J. Y.-J., Zhang, S.-Y., ... Jing, Z.-C. (2019). Germline *BMP9* mutation causes idiopathic pulmonary arterial hypertension. *European Respiratory Journal*, *53*(3), 1801609. https://doi.org/10.1183/13993003.01609-2018

Wooderchak-Donahue, W. L., McDonald, J., O'Fallon, B., Upton, P. D., Li, W., Roman, B. L., Young, S., Plant, P., Fülöp, G. T., Langa, C., Morrell, N. W., Botella, L. M., Bernabeu, C., Stevenson, D. A., Runo, J. R., & Bayrak-Toydemir, P. (2013). BMP9 mutations cause a vascular-anomaly syndrome with phenotypic overlap with hereditary hemorrhagic telangiectasia. *The American Journal of Human Genetics*, *93*(3), 530–537. https://doi.org/10.1016/j.ajhg.2013.07.004

Zhu, N., Pauciulo, M. W., Welch, C. L., Lutz, K. A., Coleman, A. W., Gonzaga-Jauregui, C., Wang, J., Grimes, J. M., Martin, L. J., He, H., Shen, Y., Chung, W. K., & Nichols, W. C. (2019). Novel risk genes and mechanisms implicated by exome sequencing of 2572 individuals with pulmonary arterial hypertension. *Genome Medicine*, *11*(1), 69. https://doi.org/10.1186/s13073-019-0685-z

SUPPORTING INFORMATION

Additional supporting information can be found online in the Supporting Information section at the end of this article.